CHALMERS

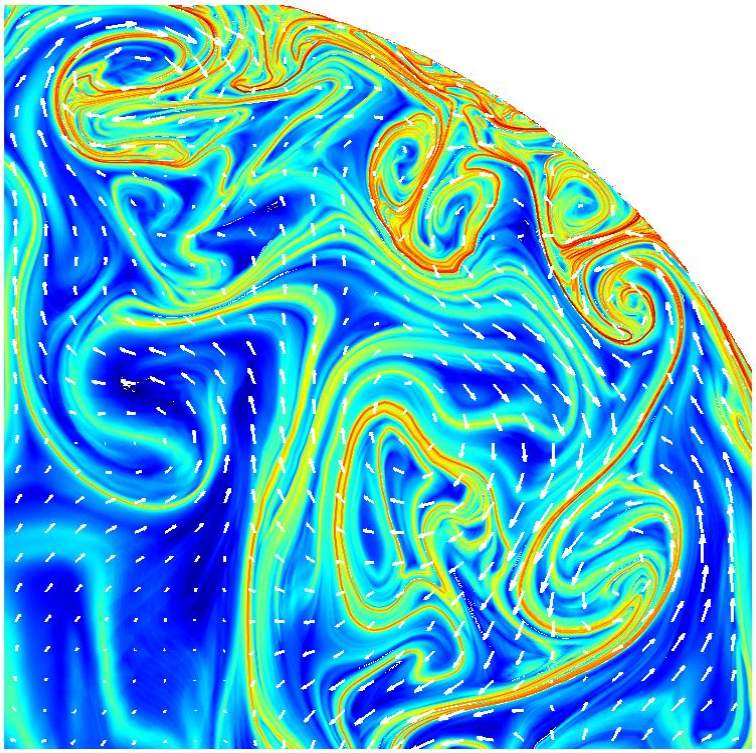

Investigation of Lagrangian Coherent Structures

- To Understand and Identify Turbulence

JOHAN JAKOBSSON

Department of Chemical and Biological Engineering
Division of Chemical Reaction Engineering
CHALMERS UNIVERSITY OF TECHNOLOGY
Gothenburg, Sweden, 2012

Investigation of Lagrangian Coherent Structures

-To Understand and Identify Turbulence

JOHAN JAKOBSSON

Examiner: Prof. Bengt Andersson

Supervisor: Dr. Ronnie Andersson

Department of Chemical and Biological Engineering
Division of Chemical Reaction Engineering
CHALMERS UNIVERSITY OF TECHNOLOGY
Gothenburg, Sweden, 2012

Investigation of Lagrangian Coherent Structures
-To Understand and Identify Turbulence
Johan Jakobsson

Department of Chemical and Biological Engineering
Division of Chemical Reaction Engineering
Chalmers University of Technology
SE-412 96 Göteborg, Sweden
Telephone: + 46 (0)31-772 1000

Cover:
The cover shows a finite time Lyapunov exponent (FTLE) field with superimposed vectors of the two space components perpendicular to the streamwise direction. More details can be found in figure 22 on page 24.

Göteborg, Sweden 2012

Investigation of Lagrangian Coherent Structures
-To Understand and Identify Turbulence

Johan Jakobsson
Department of Chemical and Biological Engineering
Division of Chemical Reaction Engineering
Chalmers University of Technology

Abstract

The finite time Lyapunov exponent (FTLE) field was calculated from advected tracer particles for various flow fields and particularly investigated for a pipe with a length of 20 cm, diameter of 5 cm and with low Reynolds number (20,000) obtained from a large eddy simulation (LES). The FTLE field was then compared to the velocity field, the turbulent kinetic energy (TKE) and an Eulerian method for identifying turbulence (the Q-criterion). It was found that the FTLE field reveals coherent structures not directly evident from instantaneous properties, e.g. the velocity field or TKE. The FTLE field has a better fit, or overlap, with TKE than the Q-criterion, yet it is not a perfect match as ridges of high FTLE values can indicate attracting or repelling coherent structures or high shear. Furthermore, the FTLE field is not in itself suitable for producing three dimensional coherent structures, rather it produces two dimensional surfaces indicating transport paths of tracer particles. Even so, enclosed three dimensional volumes might be produced by combining attracting and repelling Lagrangian coherent structures (LCS).

Keywords: finite time Lyapunov exponent, FTLE, Lagrangian coherent structures, LCS, Q-criterion.

TABLE OF CONTENTS

1 Introduction

1.1 Background

Previously prof. Bengt Andersson and Dr. Ronnie Andersson at the Department of Chemical and Biological Engineering, Division of Chemical Reaction Engineering (CRE), Chalmers University of Technology, have studied break-up of bubbles and drops in turbulent flows. It was found that single eddies interact with the bubbles and drops in order to achieve break-up (Andersson and Andersson 2006a; Andersson and Andersson 2006b). It is therefore important to be able to describe turbulence and turbulent structures in order to develop models for the interaction between eddies and particles, such as bubbles and drops. Recently at the same department Farideh Ghasempour et al. have studied the description and identification of turbulent structures using Eulerian methods (Ghasempour, Andersson et al. 2011). The research group is now interested in Lagrangian methods as a complementary and possibly an alternative way to characterize turbulent structures, and as such a method for the Lagrangian investigation of turbulent structures needs to be developed. There is also the need for more knowledge to deepen the understanding of turbulence.

1.2 Purpose

The main purpose of the project is to make a large eddy simulation (LES) of water flowing in a tube with particles injected into coherent structures and develop a Lagrangian method for investigating data generated by LES and the particle tracks in MATLAB. The particle tracks should reveal turbulent structures that can be analyzed. The goal is develop the tools needed to calculate a Lagrangian method for identifying coherent structures in order to understand turbulence, such knowledge that can be used to develop new models.

1.3 Limitations

As the main focus is to develop the method to investigate the data generated the choice of different models will not be dealt with at any deeper level. As such simulations will be performed using “best practice” guides and conventional and well tested simulation methods. The validity of LES will also not be investigated in depth but generally taken to be able to represent reality correctly for the purposes at hand. This is not to say that motivations for the choice of LES will be completely left out or that an analysis of the validity and appropriateness of LES will not be conducted at all for instance, but it is not the main focus. Furthermore, the topic of simulation methods in terms of different code packages will not be dealt with at all.

1.4 In Depth Purpose

The purpose of analyzing the data generated by Lagrangian particle tracks from velocity fields calculated through LES simulations is to be able to answer questions such as the following:

- What are the different alternatives for identifying coherent turbulent structures?
- What is the most appropriate way to determine the size of an eddy?
- How can these structures be tracked in time?
- How can the birth and death of turbulent structures be defined so that the lifetimes of eddies can be quantified?
- What distributions of lifetimes, size, turbulent kinetic energy etc. of eddies are there?

2 Method

2.1 Introduction

As stated above the purpose is to simulate water flowing in a pipe at Re = 20000, the pipe being 20 cm in length and 5 cm in diameter, the specifications of the pipe previously investigated by Farideh Ghasempour at CRE. Periodic boundary conditions will be used to make the result less dependent on initial conditions. The LES simulations will resolve the larger scales and individual turbulent structures can therefore be identified. The MATLAB program should be able to indentify coherent turbulent structures and or indentify particles belonging to the same eddy. Simulations will be performed with the ANSYS computational fluid dynamics (CFD) software Fluent. Furthermore, the large amount of data generated by LES will be analyzed and visualized with MATLAB and ANSYS Fluent.

2.2 Turbulence Modeling

The goal in modeling turbulent flows is to solve the Navier-Stokes (N-S) equations, which for a Newtonian fluid are (Andersson 2011)

$$\frac{\partial U_i}{\partial t} + U_j \frac{\partial U_i}{\partial x_j} = -\frac{1}{\rho}\frac{\partial P}{\partial x_i} + \nu \frac{\partial}{\partial x_j}\left(\frac{\partial U_i}{\partial x_j} + \frac{\partial U_j}{\partial x_i}\right) + g_i, \tag{2.1}$$

where U_i is the instantaneous velocity, t is the time, x_i is the spatial dimension, P is the pressure, ρ is the density, ν is the viscosity and g_i is the gravitational constant. In (Pope 2000) a valuable distinction between *modeling* and *simulating* equations is made. When modeling a system of equations the equations are solved for some mean or average quantity, say the mean velocity $\langle U_i \rangle$ defined as time average (Crowe 2011) at some point $\boldsymbol{x}$

$$\langle U_i \rangle(\boldsymbol{x}) = \frac{1}{T}\int_{-T/2}^{T/2} U_i(t, \boldsymbol{x}) dt, \tag{2.2}$$

where T is the averaging time. In order for the time average to be valid the averaging time must be of appropriate length, i.e. much larger than the time scale of the fluctuating velocity field and much smaller than the characteristic time scale of the large scale flow. On the other hand, a simulation of a system of equations means that the instantaneous velocity field is solved directly.

As the intended study is of phenomena occurring during very short time scales, i.e. interactions with single eddies, the solving of average properties will not suffice. Therefore we will have to look at simulation techniques. The choice thus breaks down to basically two options; direct numerical simulation (DNS) and large eddy simulation (LES) (Pope 2000; Andersson 2011; Crowe 2011). The main difference between DNS and LES is that the former simulates all scales while the latter models the smaller scales and simulates the intermediate and large scales. Because the N-S equations perfectly describe the flow and DNS computes these directly all scales of $\langle U_i \rangle$ as well as the time scales are calculated and resolved (Pope 2000; Andersson 2011). This is both the advantage and disadvantage of DNS; huge amount of data with high resolution but with large computational demand is generated. The computational cost of DNS is proportional to Re^3 (Pope 2000; Andersson 2011), however, 99% of the demand is devoted to the dissipation range (Pope 2000). The dissipation range length scale, l_0, is according to (Andersson 2011) sixty times the Kolmogorov length scale $\eta = (\nu^3/\varepsilon)^{1/4}$, where ν is the viscosity and ε is the turbulent kinetic energy dissipation rate. This together with the fact that it is only the computational cost of the smaller scales, $l < l_0$, that is proportional to Re^3 while the cost of the larger scales are only weakly dependent on Re (Pope 2000) makes LES and attractive choice. In (Andersson and Andersson 2006a; Andersson and Andersson 2006b) it is suggested that only the energy containing eddies are capable of deforming a bubble or drop to cause breakup, models of which are the very kind of phenomena this study aims to provide knowledge for, whose length scales are simulated in LES . This means that the important length scales that are of interest are still simulated even though DNS is not used and the smaller scales are modeled leading to less data and lower computational cost. In addition, the smaller scales displays more isotropy making them more suitable to model (Andersson 2011).

2.3 On Coherent Turbulent Structure Identification

There are two different kinds of methods to indentify coherent turbulent structures (eddies); Eulerian and Lagrangian. However, there is no universally accepted method of identifying a coherent structure (Haller 2005; Green, Rowley et al. 2007). Many of the Eulerian methods involve the velocity gradient tensor $\boldsymbol{\nabla} U$ (Dubief and Delcayre 2000; Chakraborty, Balachandar et al. 2005; Green, Rowley et al. 2007)

$$\nabla U_{ij} = \frac{\partial U_i}{\partial x_j}. \tag{2.3}$$

One commonly mentioned method is the Q-criterion (Green, Rowley et al. 2007), defined as

$$Q = \frac{1}{2}(\|\boldsymbol{\Omega}\|^2 - \|\boldsymbol{S}\|^2), \tag{2.4}$$

where $\|\cdot\|$ is the Frobenius matrix norm and the tensors $\boldsymbol{\Omega}$ and $\boldsymbol{S}$ are the symmetric and anti-symmetric invariants of $\boldsymbol{\nabla} U$

$$\boldsymbol{\Omega} = \frac{1}{2}\left(\boldsymbol{\nabla} U - \boldsymbol{\nabla} U^{\mathrm{T}}\right), \tag{2.5}$$

$$\boldsymbol{S} = \frac{1}{2}\left(\boldsymbol{\nabla} U + \boldsymbol{\nabla} U^{\mathrm{T}}\right), \tag{2.6}$$

where A^{T} marks the transpose of A. Coherent eddies are then defined as regions of the flow with positive values of Q and lower pressure than the immediate surroundings (Chakraborty, Balachandar et al. 2005), these can easily be visualized as isosurfaces. The Q-criterion thus identifies regions where the vorticity is stronger than the rate of strain (Haller 2005; Green, Rowley et al. 2007). Other common Eulerian methods include the Δ-criterion defined as

$$\Delta = \left(\frac{Q}{3}\right)^2 + \left(\frac{\det(\boldsymbol{\nabla} U)}{2}\right)^2 > 0, \tag{2.7}$$

and the λ^2-criterion for 2D-analysis, where $\lambda^2(\boldsymbol{A})$ is the second largest eigenvalue of a matrix $\boldsymbol{A}$ with three eigenvalues (Haller 2005), defined as

$$\lambda^2(\boldsymbol{S}^2 + \boldsymbol{\Omega}^2) > 0. \tag{2.8}$$

Which means that the Δ-criterion indentifies the cores of turbulent structures (Chakraborty, Balachandar et al. 2005) while the λ^2-criterion is a somewhat looser criterion than the Q-criterion but that guarantees local pressure minima within the 2D plane (Dubief and Delcayre 2000; Chakraborty, Balachandar et al. 2005). The drawback of the Eulerian methods is that they are not independent of the reference frame, i.e. they are not objective, and as (Green, Rowley et al. 2007) also point out they require the user to effectively chose the thresholds discretionally (as $Q > 0$ may be changed to a higher value for instance in order to more easily visualize the eddies).

To solve the problem of frame independence Lagrangian methods utilizes particle tracks of tracer particles in order to identify Lagrangian coherent structures (LCS). Perhaps the most widely used is the finite-time Lyapunov exponent (FTLE) method (Peacock and Dabiri 2010). This method relies on identifying ridges where the degree of separation, calculated by integrating in time, of different particle tracks is the greatest in order to define coherent structures. Even though this approach solves the problem of objectivity it is oftentimes computationally heavy (Peacock and Dabiri 2010). In (Brunton and Rowley 2010) the procedure for calculating the FTLE field is explained and will be restated here. If $U_i(t)$ is a flow field in three dimensions and the vector $\boldsymbol{x}(t), t \in [0, T]$, gives the position of a particle at time t with starting time t_0 and starting position $\boldsymbol{x}_0$ which satisfies the condition that the time derivative of $\boldsymbol{x}$ is equal to the velocity in the flow field at time t

$$\frac{\partial x_i}{\partial t}(t) = U_i(x_i(t), t), \tag{2.9}$$

then a flow map Φ_0^T of a finite number of particles with the above properties can be constructed, defined as

$$\Phi_0^T: \mathbb{R}^3 \longrightarrow \mathbb{R}^3; \quad \boldsymbol{x}(0, t_0, \boldsymbol{x}_0) \longmapsto \boldsymbol{x}(0, t_0, \boldsymbol{x}_0) + \int_0^T U(\boldsymbol{x}(\tau, t_0, \boldsymbol{x}_0), \tau) d\tau, \quad (2.10)$$

where $\boldsymbol{x}(t, t_0, \boldsymbol{x}_0)$ is the position of the particle with starting time t_0 and starting position $\boldsymbol{x}_0$ at time t (omitted elsewhere for simplicity). The method now aims to calculate the degree of separation, that was mentioned above, between particle trajectories and infinitesimal perturbation of the starting positions, $\boldsymbol{x}_0$, of each trajectory (Haller 2001; Shadden, Lekien et al. 2005). This is achieved by calculating the Jacobian of the flow map, $\boldsymbol{J}\Phi_0^T$, and multiplying it with its transpose which gives the Cauchy-Green deformation tensor Δ

$$\Delta = (\boldsymbol{J}\Phi_0^T)^{\mathrm{T}} \boldsymbol{J}\Phi_0^T = \left(\frac{\partial \Phi_0^T}{\partial \boldsymbol{x}}\right)^{\mathrm{T}} \frac{\partial \Phi_0^T}{\partial \boldsymbol{x}}. \quad (2.11)$$

The greatest degree of separation between a trajectory and a perturbed trajectory occurs when the starting position of the perturbed trajectory is chosen such that it is aligned with the largest eigenvector $\boldsymbol{e}_{\max}$ of Δ (Shadden, Lekien et al. 2005). Let $\boldsymbol{y}(t, t_0, \boldsymbol{x}_0)$ denote a perturbed trajectory of $\boldsymbol{x}(t, t_0, \boldsymbol{x}_0)$, then it can be shown that (Shadden, Lekien et al. 2005)

$$\max\|\boldsymbol{y}(T)\| = \sqrt{\lambda_{\max}\big(\Delta(\boldsymbol{x}_0)\big)}\boldsymbol{e}_{\max} = e^{\frac{1}{|T|}\log\sqrt{\lambda_{\max}(\Delta(\boldsymbol{x}_0))}|T|}\boldsymbol{e}_{\max}, \quad (2.12)$$

where $\lambda_{\max}(A)$ is the maximum eigenvalue of a symmetric matrix A. Finally the FTLE field is defined as the exponent in eq. (12)

$$\boldsymbol{\sigma}(\Phi_0^T, \boldsymbol{x}_0) = \frac{1}{|T|}\log\sqrt{\lambda_{\max}\big(\Delta(\boldsymbol{x}_0)\big)}, \quad (2.13)$$

Since the integration can be done in either forward or backward time the absolute value of T is needed. The choice of integration time affects the identification of Lagrangian coherent structures; forward time integration identifies ridges of repelling LCS and backward time identifies attracting LCS (Shadden, Lekien et al. 2005; Green, Rowley et al. 2007). In (Haller 2002) the direct finite-time Lyapunov exponent (DLE) is defined and the DLE field is calculated as

$$\boldsymbol{\sigma}_{\mathrm{DLE}}(\Phi_0^T, \boldsymbol{x}_0) = \frac{1}{2T}\log\big(\lambda_{\max}\Delta_{\mathrm{DLE}}(\boldsymbol{x}_0)\big), \quad (2.14)$$

which is basically equivalent to the FTLE field and the DLE method will not be investigated. In (Haller 2002) another Lagrangian method based on the Okubo-

Weiss criterion is discussed. This method is based on the same idea of particle trajectories $\boldsymbol{x}(t, t_0, \boldsymbol{x}_0)$ fulfilling eq. (9) as the FTLE method. Here, the main criterion for identifying a particle trajectory as belonging to a coherent structure is based on the determinant of the gradient of eq. (9)

$$\det\big(\boldsymbol{\nabla} U(\boldsymbol{x}(t), t)\big) > 0. \tag{2.15}$$

2.3.1 Numerical Approach of FTLE

The solution of the CFD computations will be exported as large files of data at discrete points in time and space containing velocities and velocity gradients to be read into MATLAB. The algorithm for advecting particles and calculating the FTLE field will then be:

1. Create a structured grid of particles.
2. Read the data file for the starting time step.
3. Create a linear interpolant of the velocity field.
4. Calculate velocities at particle locations.
5. Calculate the particle locations for the next time step by adding the product of the length of the time step by the velocity at the particle location to the current location.
6. Load the data file of the next time step and repeat until the final time step is reached.
7. Calculate the deformation gradient for each particle and subsequently the FTLE field.

The procedure above gives the flow map. The length of the time step will be the same as the length of the time step that have been used in Fluent. That is, the flow properties will be regarded as being constant between time steps. Note that particles can be advected both forward and backward in time which will affect in which direction the properties for a particular time step will be constant. The particles location will typically lie in between mesh grid point resulting in the need of interpolation also in space. Here a built in function of MATLAB called `triscatteredinterp.m` will be used with the linear option.

Once the flow map is obtained the Cauchy-Green deformation gradient must be evaluated. In (Shadden 2011) a method for calculating the deformation gradient from discrete data points using finite differencing is given. Let $x_{ijk}(t), y_{ijk}(t)$ and $z_{ijk}(t)$ be the positions $\boldsymbol{x}_{ijk}$ of the particle located at the vertices i, j and k of a structured grid at time t and the let the starting time be 0 and the final time be T. Then the deformation gradient can be approximated as

$$\frac{\partial \Phi_0^T}{\partial \boldsymbol{x}_{ijk}}$$

$$= \begin{bmatrix} \frac{x_{(i+1)jk}(T) - x_{(i-1)jk}(T)}{x_{(i+1)jk}(0) - x_{(i-1)jk}(0)} & \frac{x_{i(j+1)k}(T) - x_{i(j-1)k}(T)}{y_{i(j+1)k}(0) - y_{i(j-1)k}(0)} & \frac{x_{ij(k+1)}(T) - x_{ij(k-1)}(T)}{z_{ij(k+1)}(0) - z_{ij(k-1)}(0)} \\ \frac{y_{(i+1)jk}(T) - y_{(i-1)jk}(T)}{x_{(i+1)jk}(0) - x_{(i-1)jk}(0)} & \frac{y_{i(j+1)k}(T) - y_{i(j-1)k}(T)}{y_{i(j+1)k}(0) - y_{i(j-1)k}(0)} & \frac{y_{ij(k+1)}(T) - y_{ij(k-1)}(T)}{z_{ij(k+1)}(0) - z_{ij(k-1)}(0)} \\ \frac{z_{(i+1)jk}(T) - z_{(i-1)jk}(T)}{x_{(i+1)jk}(0) - x_{(i-1)jk}(0)} & \frac{z_{i(j+1)k}(T) - z_{i(j-1)k}(T)}{y_{i(j+1)k}(0) - y_{i(j-1)k}(0)} & \frac{z_{ij(k+1)}(T) - z_{ij(k-1)}(T)}{z_{ij(k+1)}(0) - z_{ij(k-1)}(0)} \end{bmatrix}. \quad (2.16)$$

Once the deformation gradient is obtained the FTLE field is straightforward to calculate from eq. (2.11)-(2.13).

2.4 Vortex Identification Criterion

To evaluate how good different methods are in identifying turbulence requires some objective measure. This work will utilize a concept described in (Ghasempour, Andersson et al. 2011). The assumption is that the turbulent kinetic energy (TKE) of a flow should be wholly contained in the turbulent structures themselves. The turbulent kinetic energy k for a three dimensional system is defined as (Andersson 2011)

$$k = \frac{1}{2}\langle u_i u_i \rangle = \frac{1}{2}(\langle u_1^2 \rangle + \langle u_2^2 \rangle + \langle u_3^2 \rangle), \quad (2.17)$$

where u_i is the velocity due to turbulence. The decomposition of the velocity, termed U_i, used in LES is (Garnier 2009; Andersson 2011)

$$U_i(\boldsymbol{x}, t) = \overline{U}_i(\boldsymbol{x}, t) + u_i'(\boldsymbol{x}, t), \quad (2.18)$$

where $\overline{U}_i$ is the velocity of the resolved large scales andu_i' is the velocity of the sub grid modeled scales. With the average velocity $\langle U_i \rangle$, see equation (2.2), the different velocities can be related by

$$u_i = U_i - \langle U_i \rangle = \overline{U}_i + u_i' - \langle U_i \rangle. \quad (2.19)$$

The method thus compares the turbulent kinetic energy captured by an identification scheme to the total TKE in the flow. This is achieved by the ratio of the TKE inside the volumes of turbulent structures to the total TKE.

A benchmark for this method that will be used is the Q-criterion for the Lamb-Oseen vortex that was calculated in (Ghasempour, Andersson et al. 2011) and will be restated here. The tangential velocity for the Lamb-Oseen vortex can be written (Devenport, Rife et al. 1996)

$$U_\theta = U_{\theta 1}\left(1 + \frac{0.5}{\alpha}\right)\frac{r_1}{r}\left[1 - exp\left(-\alpha\frac{r^2}{r_1^2}\right)\right], \tag{2.20}$$

where U_θ is the velocity in the tangential direction, $U_{\theta 1}$ is the peak tangential velocity, $\alpha = 1.25643$ is a constant, r is the radius from the center of the vortex and r_1 is the core radius defined as

$$r_1(t) = \sqrt{4\nu t}, \tag{2.21}$$

where ν is the viscosity of the fluid and t is the time. The vortex will dissipate away due to viscosity and the time dependence of the core radius. A plot of velocity vectors for the Lamb-Oseen vortex can be seen in figure 2 below, and from the figure it can be seen that the magnitude of the velocity is constant for a given radius. Given that the TKE is proportional the square of the fluctuating velocity and that a vortex is that fluctuation the TKE of the Lamb-Oseen vortex is given by squaring the velocity field directly. A plot of TKE and the Q-criterion can be seen in figure 1 below. The amount of TKE captured by the Q-criterion is about 28 % of the total TKE up to a radius of 0.025 m and the cutoff is at the core radius.

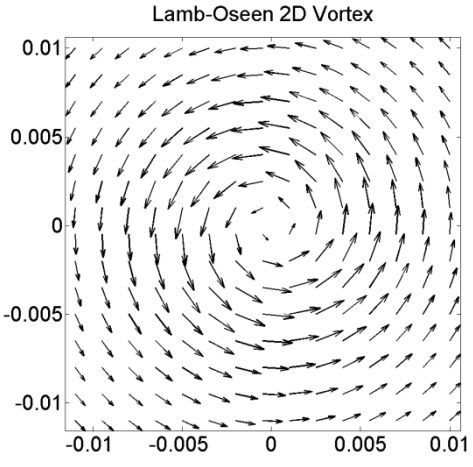

Figure 2. Plot of velocity vectors for a Lamb-Oseen vortex with α=1.25643, $U_{\theta 1}$=0.25 m/s, υ=0.001003 Pa·s (water) and t=0.006231 s.

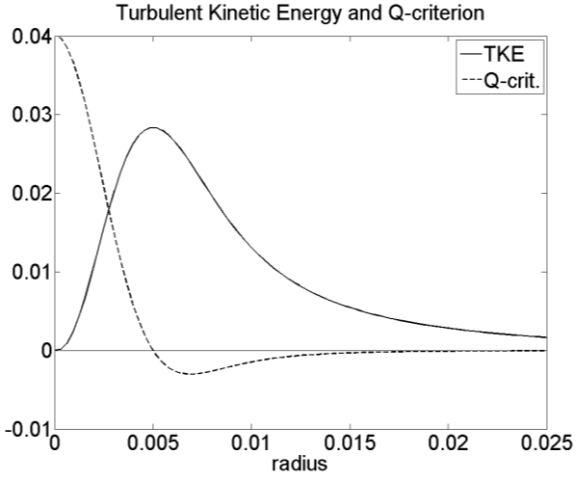

Figure 1. Plot of TKE and Q-criterion as a function of the radius, the benchmark cutoff is at about 28 % of the total TKE. The values of the Q-criterion have been rescaled by a factor of 5.2e-6 to fit in the same window.

It is thus desirable to find a method that captures more than 28 % of the total TKE in order to be able to give a better description of turbulence.

3 Results

3.1 FTLE of Some Analytical Functions

The approach of revealing turbulent structures by particle trajectories was initially tested on a few analytical equations aimed at describing two dimensional flows in order to make sure that the MATLAB code performs well.

3.2 Time-variant Double Gyre

Initially the FTLE fields were calculated for a standard case that is used in the literature (Shadden, Lekien et al. 2005; Brunton and Rowley 2010). The double gyre flow field is defined in a domain $\Omega: \{x \in [0,2], y \in [0,1]\}$ by the stream function ψ

$$\psi(x, y, t) = A \sin(\pi f(x, t)) \sin(\pi y), \tag{3.1}$$

$$f(x, t) = a(t)x^2 + b(t)x, a(t) = \varepsilon \sin(\omega t), b(t) = 1 - 2\varepsilon \sin(\omega t), \tag{3.2}$$

where ε and ω are constants. To get the velocity field the gradient is utilized

$$u_x = -\frac{\partial \psi}{\partial y}, u_y = -\frac{\partial \psi}{\partial x}. \tag{3.3}$$

The velocity field is plotted at three different time instants in figure 4 below, from which an oscillating nature of the line of separation of the two gyres is evident. The FTLE field is plotted in figure 3 below. Here the particles were tracked backwards in time revealing *attracting* Lagrangian coherent structures (aLCS).

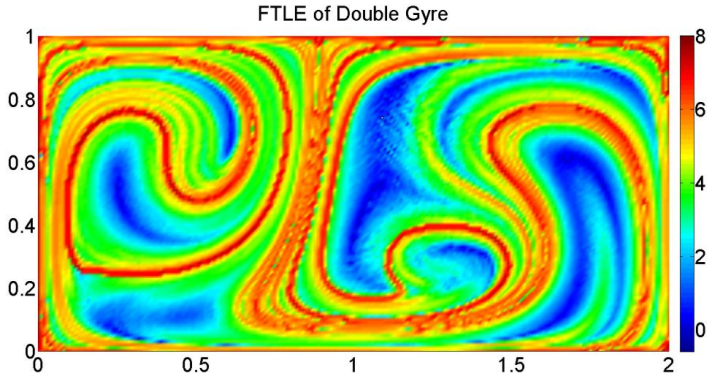

Figure 3. The FTLE field of the double gyre at $t = 0$. Here $A = 0.1, \varepsilon = 0.25$ and $\omega = 2\pi/10$ has been used, these specifications apply to all double gyre FTLE plots. The integration time was $T = -20$. The ridges of highest FTLEs separates the aLCS.

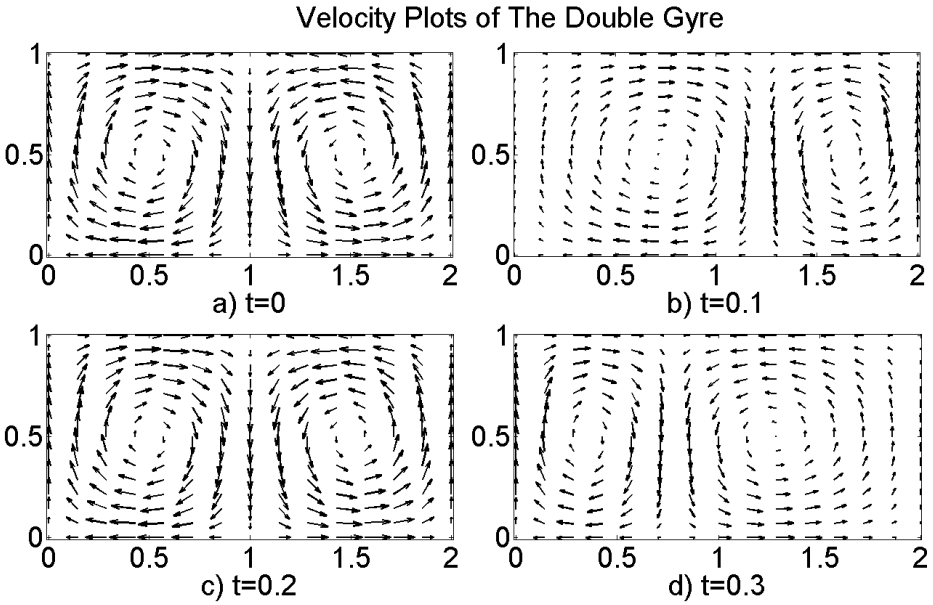

Figure 4. Four plots at different times that show the time dependence of the double gyre. Here $A = 0.1, \varepsilon = 0.25$ and $\omega = 2\pi/10$ has been used. The plane of separation between the two gyres oscillates with frequency $\omega/2\pi$ and is displaced a distance approximately equal to ε (Shadden, Lekien et al. 2005).

The time evolution of the FTLE field was studied and tracer particles were followed simultaneously. In figure 5 the FTLE field and current positions of a few tracer particles are plotted at consecutive time steps.

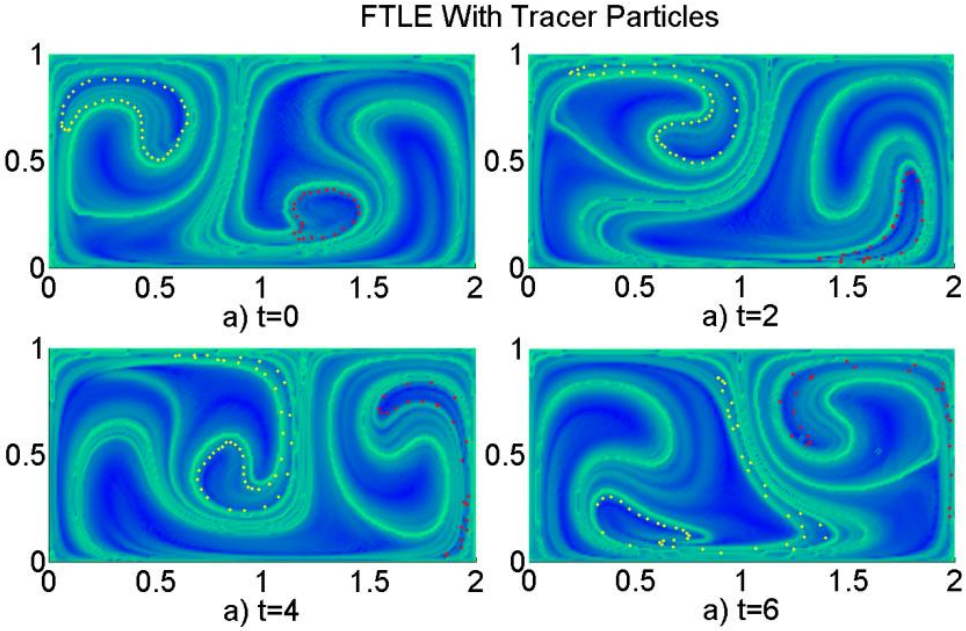

Figure 5. Plot of tracer particles injected at $t = 0$ s and snapshots at $t = 2$ s, $t = 4$ s and $t = 6$ s with the corresponding backward time (integration time $T = -20$ s) FTLE field. The particles are injected into two differenc aLCS and by time $t = 4$ s it can be seen that both vortices are leaving a trail of particles behind while other particles are still contained within the vortex.

When integrating, or advecting, particles forward in time *repelling* LCS (rLCS) are revealed. In figure 6 the FTLE field of rLCS is plotted.

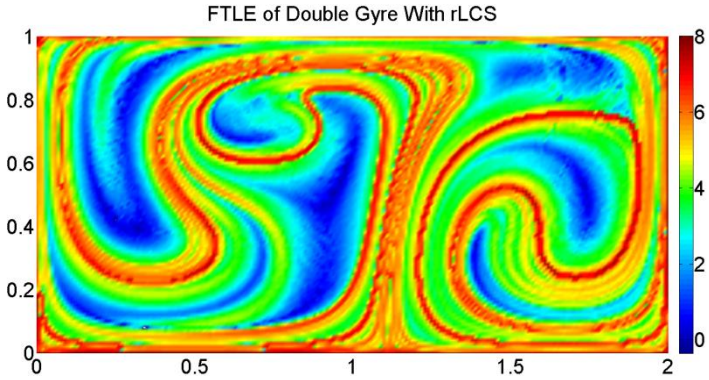

Figure 6. Plot of the FTLE field of rLCS. The same specifications as in figure 3 apply here excepts that the integration time is $T = 20$ s.

When the ridges of highest FTLE for the rLCS are extracted and plotted on top of the FTLE field of aLCS sections vortices are divided into parts that will leave the structure at different time scales. Figure 7 shows the FTLE field of aLCS with ridges of rLCS on top of it and figure 8 shows snapshots of particles injected into different section of an aLCS at consecutive time steps.

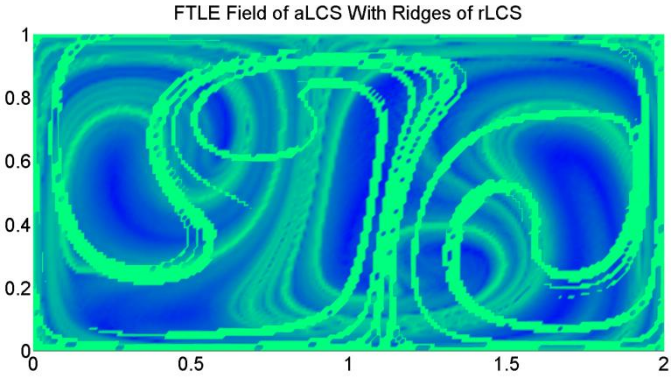

Figure 7. Plot of a FTLE field with aLCS and ridges of repelling ridges (material lines) in top of it to indicate what sections of certain attracting structures will be transported together.

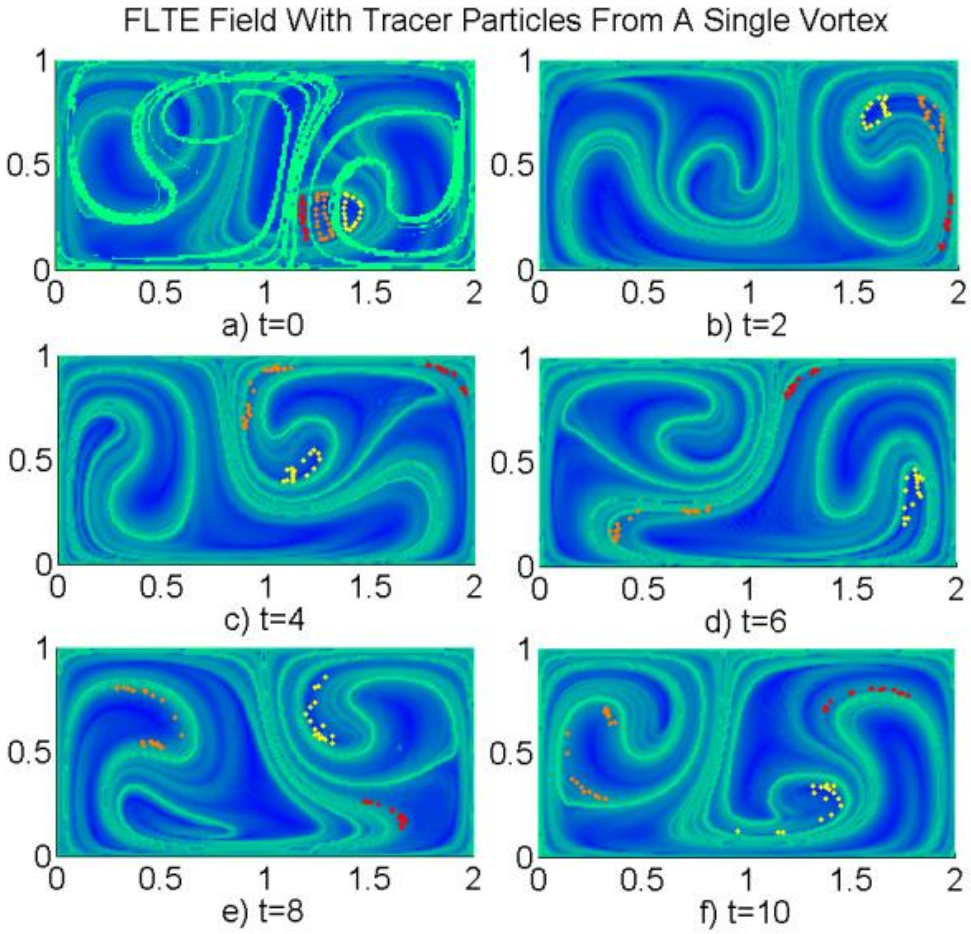

Figure 8. Plot of tracer particles at consecutive time steps after having been injected into three different sections of an aLCS divided by ridges of high FTLE values (>64 % of max). Initially at time $t = 0$ s all particles (yellow, orange and red) are contained in the vortex. First to leave are the red particles, approximately at $t = 2$ s, and soon afterwards the orange particles as well at $t = 4$ s. At the last time step plotted, $t = 10$ s, particles of different colors are contained in wholly different vortices with only yellow particles in the original vortex where some of them have started to trail behind.

3.3 FTLE of Lamb-Oseen Vortex

The Lamb-Oseen vortex described in section 2.4 was first considered for a case without the time dependence of the core radius. The core radius was set to $r_1 = 0.005$ m. Furthermore, several interacting vortices were introduced by overlapping velocity fields of Lamb-Oseen vortices with vortex centers located near each other in different constellations. In figure 9 the FTLE field of three vortices placed in a triangle with equal sides is plotted.

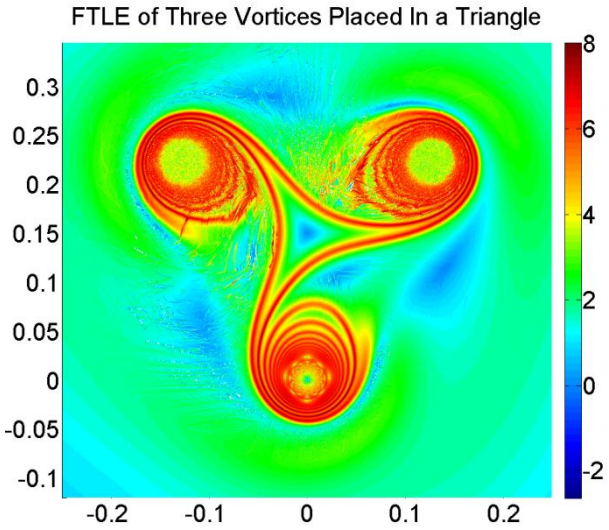

Figure 9. Plot of three Lamb-Oseen vortices whose vector fields have been superimposed. The distance between the different vortex centers is 29 cm. A pseudo steady state core radius was used for this case.

The LCS indentified depends on the distance between vortex centers and the arrangement of the vortices. In figure 10 the FTLE field of three vortices in line is plotted.

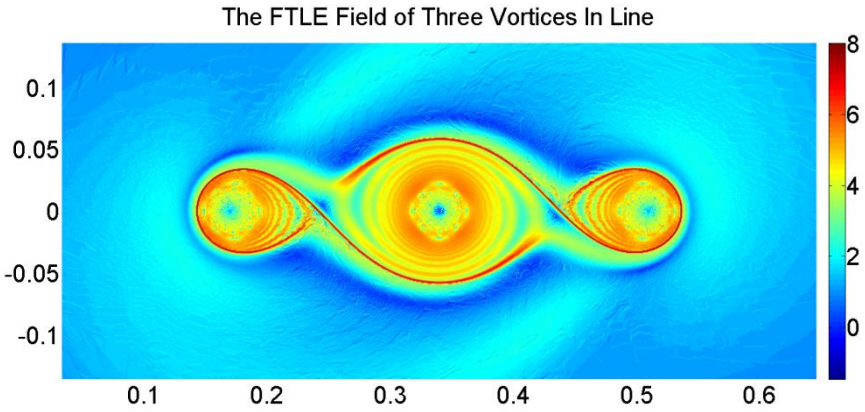

Figure 10. The FTLE field of tree Lamb-Oseen votrices in line. The regions identified as coherent are of unequal size when comparing the vortex in the middle to those to the right and left eventhough they have the same velocity field functions. Integration time was $T = -20$s.

When the FTLE field from a single Lamb-Oseen vortex is calculated no coherent structure can be discerned. This is the result of the fact that at no point in the velocity filed does two neighboring advected particles end up very far from each other. In order for advected particles to be able to indentify coherent turbulent structures there must be two or more Lamb-Oseen vortices present. This also results in the fact the shape and size of the LCS depends on how the different vortices are places in relation to each other. In figure 11 the FTLE field of three vortices placed in the same arrangement as those in figure 9 is plotted. It

can be seen that shape is more round and the size is larger compared to the LCS identified in figure 9b. Also in figure 11 a comparison is made between integrating forwards and backwards in time. This produces similar structures, the difference being that the rotation is opposite, since revering the time is equal to reversing the rotation the same time direction.

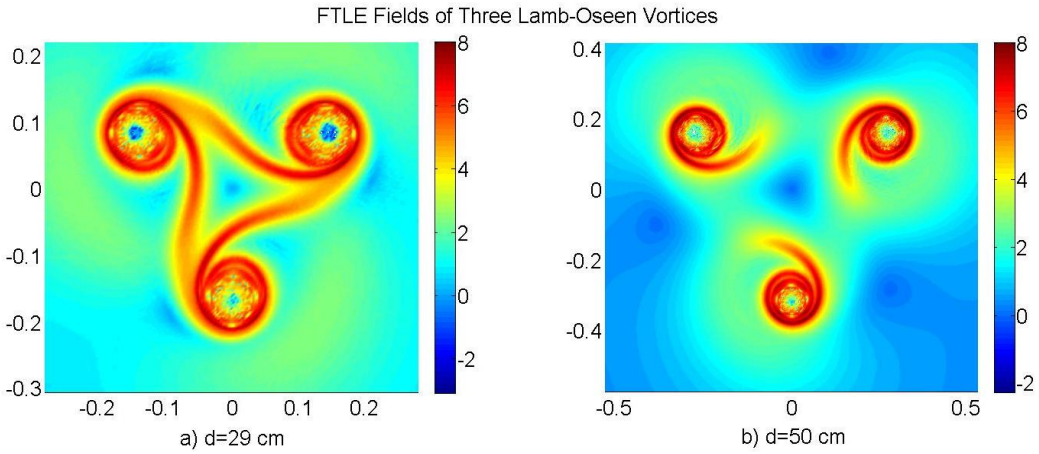

Figure 11. Three Lamb-Oseen vortices superimposed at a distance of $d = 29$ cm in a and 50 cm in b. In a the integration time was $T = -20$ s and in b $T = 20$ s. The shorter distance show more interaction in a. It is worth noting the reversed direction of the ridges as reversing time is equal to revering the flow direction in the same time direction.

For water the Lamb-Oseen vortex dissipates rather quickly so that the transient core radius term makes the vortex dissipate rather quickly. A transient core radius was therefore considered for a fictitious fluid with very low viscosity, i.e. $\mu = 3 \cdot 10^{-7}$ Pa·s, such that the vortex is the strongest at approximately time $t = 20$ s. Repelling LCS could then be calculated by advecting particles forward in time with integration time $T = 20$ s. In figure 12 below the rLCS in the FTLE field can be seen for three vortices placed in a triangle with equal sides $d = 29$ cm. The shapes of the LCS in figure 12 are slightly oval; however, to find some value to compare to the performance of the Q-criterion the radius at a certain location of a LCS was measured. Vector fields of three vortices placed in the same way as in figure 12 with different spacing were investigated. The radius of the lowest placed vortex in the negative y-axis direction for $x = 0$ was measured. The radius was measured by injecting particles near the ridge of the LCS and tracking them to see which rotate only around the vortex enclosed by the LCS-ridge. In figure 13 the way particles were injected can be seen and in table 1 the results.

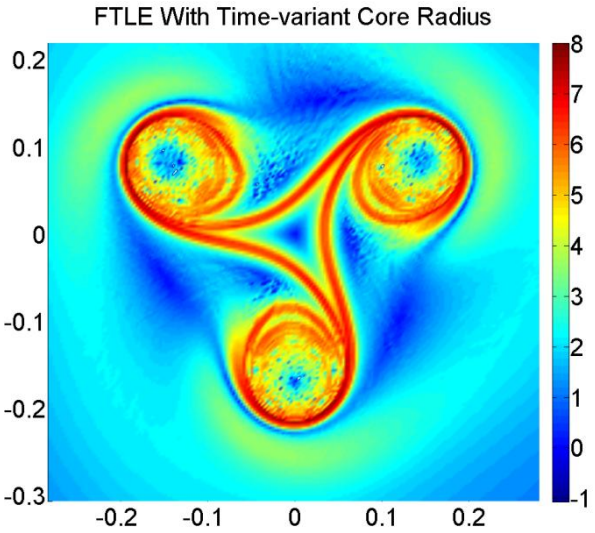

Figure 12. Plot of FTLE field for the double gyre with a distance of $d = 29$ cm between vortex centers and with particles advected forward in time (integration time $T = 20$ s) revealing repelling LCS.

It was found that the largest distance from the center of the vortex at which a particle could be injected and still remain within the LCS surrounding the vortex center, here defined as the *coherent radius*, was a constant fraction of the distance d separating the three vortex centers.

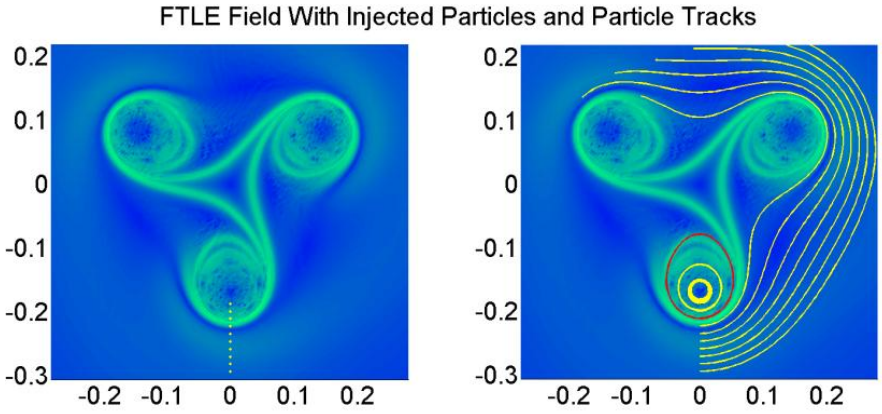

Figure 13. Plot of particles injected and advected forward in time to determine the exact radius at a specific location on the ridge of the LCS. The left figure shows the injection location. The right figure shows the particles tracks, the red track indicates the track of the particle that was injected furthest away from the vortex center and still belonged to the LCS. To get more accurate results more new particles were injected around the starting point of the red track with more densely location particles.

Table 1. The results of measuring the coherent radius show that the coherent radius is a function of the distance d between vortices.

Distance d [cm]	coherent radius r [cm]	r/d
13.9	2.08	0.1500
29.4	4.42	0.1500
34.6	5.20	0.1500
45.0	6.76	0.1500
62.4	9.36	0.1501

For comparison the FTLE field and Q-criterion was calculated for three vortices located at a distance of $d = 5.2$ cm apart from each other. Again a fictitious fluid with very low viscosity was used, $\mu = 3.3 \cdot 10^{-7}$ Pa·s, and the particles were injected at time t= 20 s, and the Q-criterion was also calculated that time, and advected forward in time, T= 20 s. The result is plotted in figure 14 below.

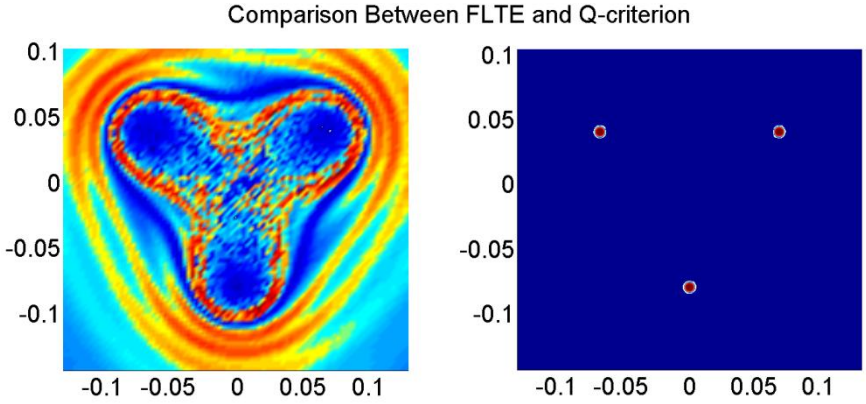

Figure 14. The two plots illustrate the difference between FTLE and Q-criterion for identifying coherent regions. The vortex centers are located a distance $d = 13.9$ cm apart. The two methods give quite opposite results; the Q-criterion give a picture of three small independent vortices far apart while the FTLE filed show large structures with strong interactions.

3.4 FTLE from CFD Solution Data

3.4.1 CFD Simulation

The simulations were performed within the ANSYS Workbench environment. The domain was a pipe with length $l = 20$ cm and diameter $d = 5$ cm with periodic boundary conditions for the "inlet" and "outlet". The wall had a no slip boundary condition. The medium in the pipe was water with an average speed of $u = 0.4$ m/s. This gives a Reynolds number of Re$= 1000 \cdot 0.4 \cdot 0.05/10^{-3} =$

20,000. To start up the calculations a stationary k-ε model was used and because of the Reynolds number the low Re k-ε was chosen. When a reasonably converged solution was obtained the model was changed to a Large Eddy Simulation (LES) model. For the sub grid scale model the Smagorinsky-Lilly model was chosen. The simulation was then carried out with a time step of $t_{step} = 0.001$ s and the solution was advanced for about 4000 time steps to obtain a "stationary" behavior of the flow and then the solutions for time steps between approximately 4300 and 5300 was exported and used to calculate FTLE fields in MATLAB. About 82 % of the turbulent kinetic energy was resolved on a relatively coarse structured mesh of 407,900 cells. The resolution in the streamwise direction was 2 mm and the average side length in the wall normal direction was 0.69 mm. To save computational time smaller sections of the pipe was chosen for calculations of the FTLE field. In order to find an interesting region the Q-criterion of the entire pipe was studied and such a plot can be seen in figure 15.

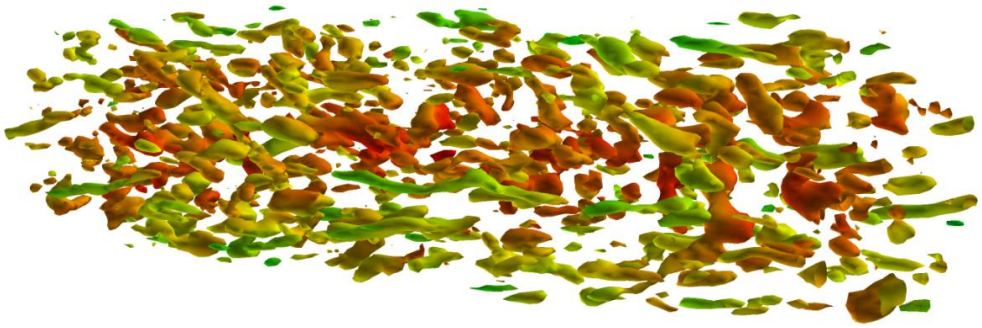

Figure 15. Plot of iso-surfaces of the normalized Q-criterion for a value of $Q_n = 0.21$. The vortices are colored by velocity magnitude.

One vortex that was identified by the Q-criterion was located in the domain $\Omega \in [-13,1] \times [-21,-7.5] \times [110,145]$ mm, illustrated in figure 16.

Figure 16. Plot of iso-surface of a vortex contained in the domain $\Omega \in [-13,1] \times [-21,-7.5] \times [110,145]$ mm, for which a FTLE field was calculated. The vortex is colored by velocity magnitude.

3.4.2 FTLE Field

The FTLE field was calculated with the Matlab code attached in Appendix A1. In figure 17 the surface plot of a cross section with constant z-value of the

domain $\Omega \in [-13,1] \times [-21,-7.5] \times [110,145]$ mm, described in section 3.4.1 above, is shown together with a surface plot of the same area with the Q-criterion for comparison. In figure 18 the FTLE field of a cross section of the whole pipe at the same z-value is shown.

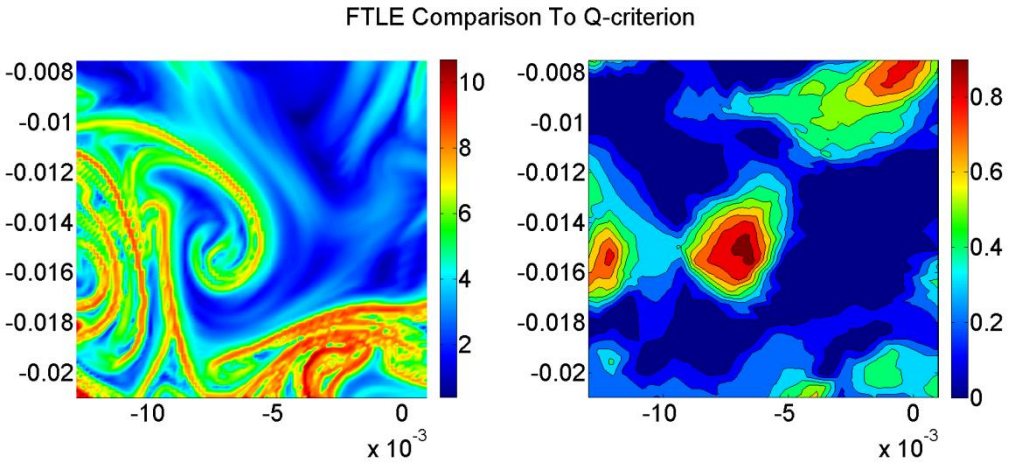

Figure 17. The surface plot of a cross section of the domain $\Omega \in [-13,1] \times [-21,-7.5] \times [110,145]$ mm at $z = 12.96$ cm; shown with a FTLE field on the left and the normalized Q-criterion on the right. The FTLE field was calculated with an integration time $T = -0.5$ s (500 time steps).

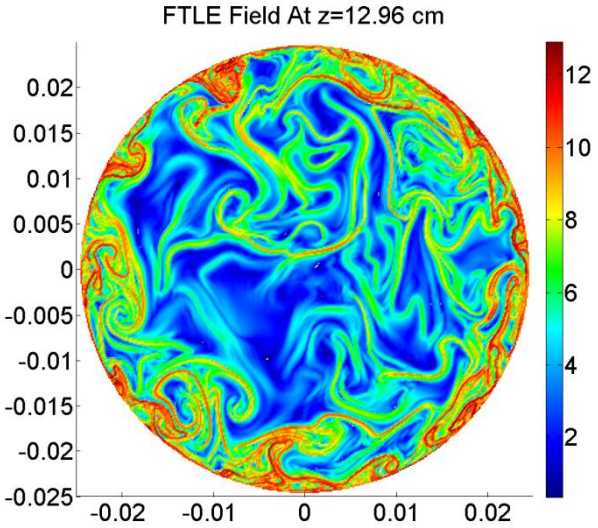

Figure 18. The FTLE field of a cross section of the entire pipe at $z = 12.96$ cm is showing attracting LCS. It can be seen that the vortex studied in figure 18, seen here around the point (-0.01,-0.015), is possibly paired with another vortex to the left which is not indicated from the Q-criterion. The integration time was $T = -0.5$ s (500 time steps).

In the mesh produced in Ansys for CFD calculations had 4180 grid points for a cross section of the pipe. However, the number of particles needed to get a high

resolution FTLE field can be much higher. For comparison, in figure 19 and 20 the FTLE field of high and low resolution respectively is plotted. It can be seen that no additional structures are revealed, only the detail is improved. Another difference is the value of the FTLE ridges, with higher resolution the FTLE ridges will have higher peaks and they will also be narrower.

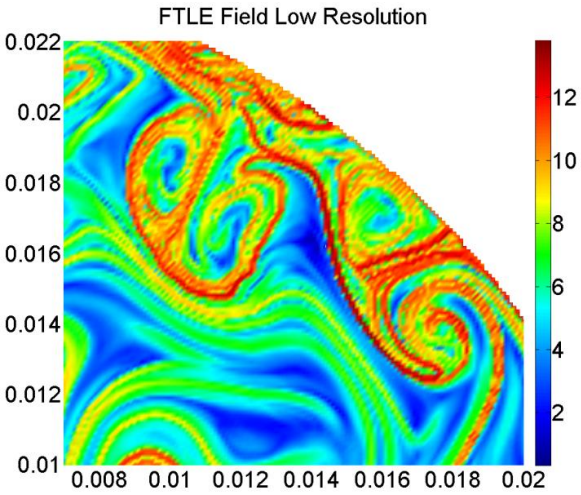

Figure 20. The resolution of the FTLE field is 188,549 particles per cross section

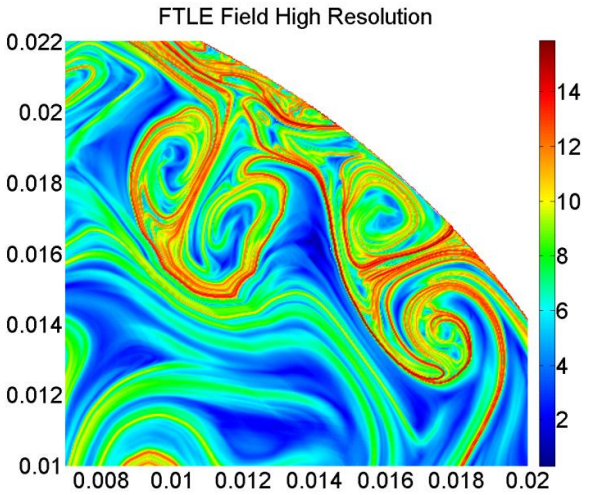

Figure 19. The resolution of the FTLE field is 2,095,237 particles per cross section.

The overlap of the FTLE field to that of the turbulent kinetic energy (TKE) and the velocity field was also studied. In figures 21 and 22 the comparison between FTLE and TKE and FTLE and the velocity field respectively for a cross section is plotted.

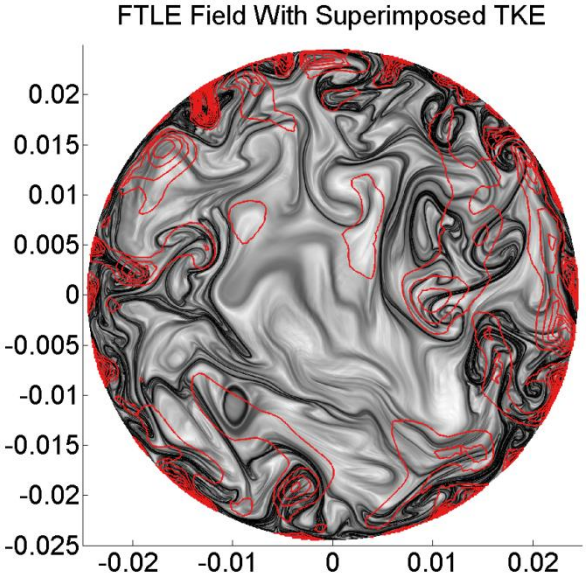

Figure 21. The figure shows a FTLE field of aLCS with iso-levels of turbulent kinetic energy. The gray scale indicates FTLE values and the red iso-lines TKE (compare fig. 24).

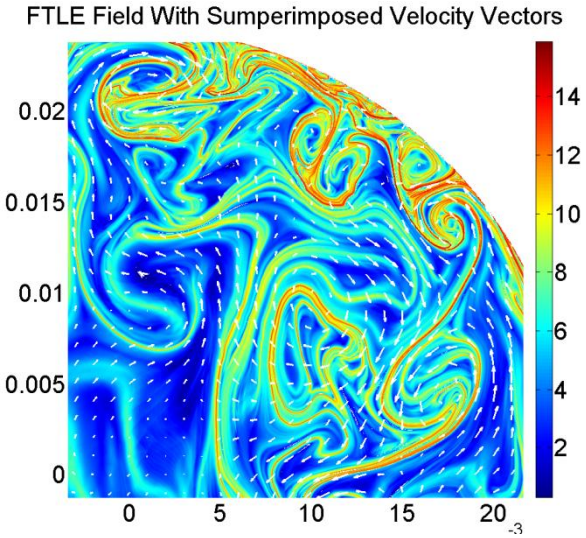

Figure 22. The forward time FTLE field with the x and y components of the velocity field superimposed. The x and y components are perpendicular to the streamwise component z.

4 Discussion

4.1 Double Gyre Example

The main purpose for studying this flow field was to begin to develop the MATLAB code and approach to calculating FTLE fields and to get a basic understanding of Lagrangian coherent structures. The results of (Shadden, Lekien et al. 2005; Brunton and Rowley 2010), where among other flow fields that of the double gyre is studied, could be replicated in the results section 3.2, e.g. see figure 3. The results also show that the FTLE fields are a powerful tool for describing the flow and transport phenomena not revealed by the instantaneous properties, such as the instantaneous velocity field or Eulerian measures as the Q-criterion. The FTLE field shows which locations where particles are moving together and where the transport of particles in and out of the LCS is taking place as is evidenced by figure 5. It could also be established which locations of particles of a LCS that will stay together for a longer period of time, i.e. where most of the transport in and out of the LCS is taking place. Figure 8 show that repelling LCS (rLCS) reveals which parts of the attracting LCS (aLCS) will stay together longer during the time evolution of the aLCS.

4.2 Lamb-Oseen Vortices

The purpose of studying the Lamb-Oseen vortex was to some extent to further test the method, however the main purpose was to deepen the understanding of LCS. No previous work has been indentified on LCS applied to the Lamb-Oseen; yet, it cannot be assured that this is because of its non existence. However, this led to a rather unexpected result, namely that a single Lamb-Oseen vortex is not identified as a LCS, i.e. a LCS with sharp ridges as opposed to slowly varying height of the ridges (the use of “sharp ridge” is not defined

rigorously, it is has a qualitative meaning here). The realization that several vortices are needed is quite telling about the nature of LCS, if a sharp ridge is to exist two neighboring particles must have markedly different end locations when advected by the flow. The reason that a single vortex does not produce a LCS with sharp ridges is because the equations governing the flow are only describing the turbulent velocity and not the entire velocity field, i.e. the equivalent of the fluctuating velocity of the Reynolds decomposition (see equation 2.18). In the case of the Lamb-Oseen vortex the turbulent velocity slowly dies out as the radius from the vortex center is increased making the difference in final position of adjacent particles trajectories decrease in the same manner and no sharp ridges are formed. If a bulk flow was present this would likely not be the case as the ratio of the turbulent velocity, or the fluctuating velocity, to the mean velocity would flatten quite fast past the core radius (see equations 2.20 and 2.21), i.e. the turbulent velocity would be completely damped in the bulk.

Rather than constructing a mean velocity field, that arguably would have to been constructed in three dimensions, to work around the problem of not producing sharp edges several vortices were introduced. By simply introducing several, in this case three, vortex centers particles tracks became more complex. When there are three vortex centers, with their respective velocity field added to each other, some particles will rotate only around one vortex while others will rotate around all three vortices. This leads to the formation of very sharp edges of the FTLE field and coherent structures can be identified. However, since the Lamb-Oseen vortex is dissipated by viscosity the dissipation rate can be too high if the viscosity is not very low in order to produce sharp ridges. Therefore a “pseudo steady state” approximation without the dissipation was initially studied. From figures 9 and 10 (see p. 15) it can be concluded that the shapes LCS depends on the interaction between different vortices, i.e. how the different vortex centers are placed in relation to each other.

It was also found that not only the placement of vortices in terms of the formation but also the distance had an influence, to some extent in shape but largely in size. For vortices placed in a triangle the coherent radius in one direction was found to be about 15 % of the distance between vortex centers, see figure 13 and table 1. One can speculate that this dependence would disappear for larger distances if a bulk flow was present as the interaction would not be significant at larger distances, yet, the coherent radius would then depend on the strength of the bulk flow. This leads to the regrettable inability of the FTLE method of producing an “objective” cut off criterion for a coherent region for the Lamb-Oseen vortex, like the one for the Q-criterion (see figure 1), that was sought after. That is, the region defined as coherent by the FTLE field is not really dependent on the coherent radius like the Q-criterion is. This is in a way a rather surprising conclusion and brings into question what a turbulent structure really is or how it should be *defined*. The Q-criterion seems to suggest that turbulence consists of basically individual rotating cylinders of varying size and energy that are largely independent of each other in terms of the definition of their respective coherent structures. This lead to the conclusion that if a cloud of

tracer particles were to be injected into such a structure they should on the most part during the life time of the structure remain within it, i.e. the fluid elements should be same. The picture painted by the FTLE method is in contrast to the one of the Q-criterion, the difference in size and interaction is obvious from figure 14. The differences in the FTLE view that can be concluded from the Lamb-Oseen vortex is that the shape and size of turbulent structures depends on all vortices present in the flow field. However, there are similarities as well; turbulence can still be thought of as structures of rotating cylinders, even if they influence each other. Yet, that is how the Lamb-Oseen vortex is constructed, so it is not surprising. Therefore, with the aid of CFD calculations, it will be seen how the divide between the Eulerian and Lagrangian views is bridged or further distinguished in the next section.

4.3 CFD Calculated Vortices

In this work the velocity field and the vortices obtained from CFD solutions of the Navier-Stokes equation are taken to more or less accurately describe real turbulence. The FTLE fields that were calculated shed light on what a turbulent structure is. The gap that was created by study of the Lamb-Oseen vortex is now widened. The results of the FTLE fields obtained from vortices calculated by solving the N-S equations not only show strong interaction, by adjoining FTLE ridges, between closely located vortices but the general shape is different. The clear pictures of the Q-criterion is muddied even further, not all coherent structures found be the FTLE method have clear boundaries. Rather than being three dimensional volumes of coherent regions they are generally two dimensional surfaces. This indicates that in some regions of the coherent structures there is a constant transport of fluid elements, some are being left behind and some are being engulfed. That is, the fluid elements that make up the turbulent structures are not constant in any discernible time frame but are dynamically changing. However, there are still coherent boundaries separating the vortices. Figure 17 (p. 20) shows the discrepancy between the two views, even though they both show a structure in middle, the one showed in its entirety in figure 16 by the Q-criterion, and some corresponding structures around it, still, there is a structure in the upper left corner by the Q-criterion that is not reproduced in the FTLE field. In figure 23 below the two methods are compared for a cross section of the pipe.

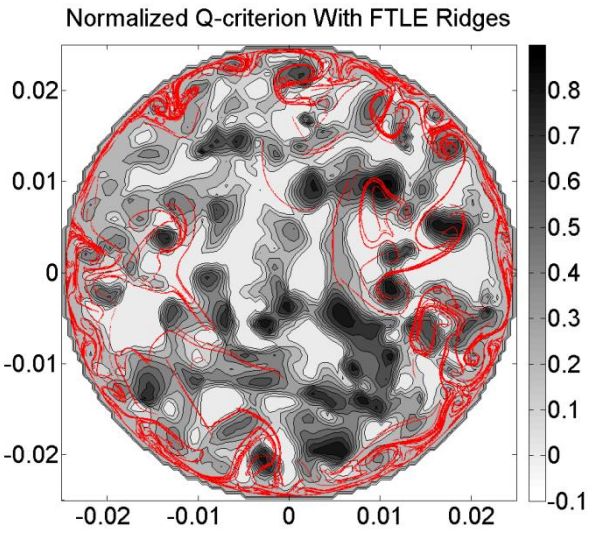

Figure 23. The figure shows a cross section of filled contours of the normalized Q-criterion with superimposed ridges of FTLE values larger than about 60 % of max.

It can be seen that the two methods do not correlate completely and that there are discrepancies between the two. However, there are also overlaps and for some vortices great similarities.

The FTLE field shows rather good overlap for turbulent kinetic energy as seen in figure 21 on page 21. This is an improvement from the Q-criterion; in figure 24 the normalized Q-criterion with iso-levels of TKE can be seen for comparison.

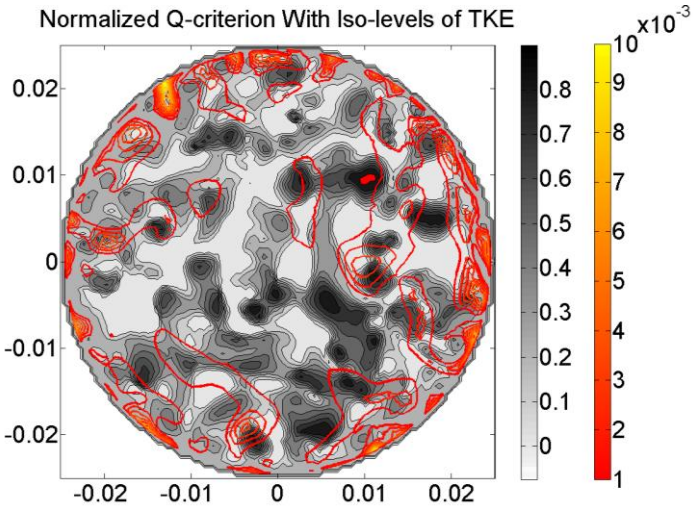

Figure 24. The figure shows the normalized Q-criterion with iso-levels of turbulent kinetic energy. The gray scale indicates Q-values and the colored scale TKE [m^2/s^2].

Still, even if the overlap seems better for the FTLE field it is not perfect; there are instances of high TKE but no apparent structure and there are structures even though the TKE is not peaking over it. Even so, there are some striking overlaps for the FTLE method that does not seem as prevalent for the Q-criterion.

The goal of constructing three dimensional structures from calculated FTLE fields, so that for instance the amount of TKE captured by the method could be calculated, is not feasible without constructing some additional criteria on how to extract these volumes from what essentially are two dimensional surfaces. One such strategy, which is described in (Shadden, Dabiri et al. 2006; Olcay and Krueger 2008), looks at the enclosed volume between attracting and repelling LCS. This approach can have difficulties, by examination of figure 8 on page 14 concerning FTLE fields of the double gyre it is clear that the structure is not divided into a single volume, or area rather as this is two dimensional, but three which can lead to ambiguity. Another difficulty in general for determining coherent structure is that the ridges of the FTLE field can be quite close together and separate at times and then be adjoined at other places. The difficulty arises in interpreting if this is an indication of several separate structures or due to numerics or perhaps gradients within a single coherent structure. According to (Haller 2011) the ridges of the FTLE field of three dimensional flows show surfaces of locally the strongest attraction, repulsion or shearing surface. Haller has also developed a mathematical method to distinguish them. This could further rule out some ridges, even so, no three dimensional surfaces would appear. However, this explains the fact that the turbulent kinetic energy is not completely in accordance with the FTLE field. This is a topic to study if further investigation, to continue the present work, should be conducted in the future.

Even if it is the case that the Lagrangian method of FTLE is not a complete match with the Eulerian methods is not at odds with other research in the field. In (Green, Rowley et al. 2007) the FTLE method is compared to some Eulerian methods and the same result is found, the different methods do find different structures as is the case in this work. Green et al. point out that Eulerian methods rely on derivatives of the velocity field that is claimed to often be noisy, which could explain some of the discrepancy, and that the Lagrangian methods do away with having to deal with user defined thresholds. What is meant here is for instance that for the normalized Q-criterion a value, typically between 0.1 and 0.5, needs to be arbitrarily chosen by the user in order to define the coherent structures. What has been found in this work is that a similar threshold is also needed for the FTLE method, namely when extracting ridges a threshold of the maximum value needs to be chosen in a similar manner.

When calculating FTLE field a grid of particles is advected that typically is denser than the grid of the solution data of the velocity field being studied. As commented in (Green, Rowley et al. 2007) the level of detail that can be obtained from FTLE fields is greater than that of Eulerian methods. This is a drawback as well as an advantage since more computational effort is required

when calculating FTLE fields. Yet, the level of resolution will not affect the size and location of coherent structures as evidenced by figures 19 and 20 on page 21.

5 Conclusions

The purpose of the present work was to look into the method of Lagrangian particle tracking in order to indentify turbulence. It was soon realized after consulting the literature that finite time Lyapunov exponents (FTLE) method was the most widely used and therefore most appropriate for the purposes at hand in terms of finding documentation on how to use it and to be able to compare results with. The FTLE method was then investigated for three types of flow; a double gyre, the Lamb-Oseen vortex and finally for a CFD calculated LES simulation of a turbulent pipe flow.

It was found that the FTLE field indeed shows structures that are not apparent when studying the instantaneous properties of the flow. Results in the literature regarding the double gyre could be replicated. And the behavior of particles was predicted by the FTLE coherent structures. Furthermore, the most important finding was that of the very definition of turbulent structures. Are they three dimensional structures as suggested by Eulerian methods or are they largely two dimensional surfaces indicating a more dynamic picture. The FTLE method of describing turbulence thus seems to suggest that turbulent structures should be considered as structures whose properties and fate not only depends on their inherent properties bur also on other structures in the vicinity as well. That is, if certain properties of coherent structures were to be determined for predicting the future of the structure some of them would be independent on the structure itself, in terms of size, energy etc., as they would depend on the surrounding structures. The failure of the FTLE method to produce three dimensional coherent structures, at least in this work, might be related the procedure of calculating the FTLE field. Since the particles are advected for a total of half a second that time period is influential on what structures one find. It might be the case that only the most stable part of the coherent structures get captured and that the some parts are changing direction and location too fast for the FTLE field to capture the behavior. This also means that the integration time is important. Vortices located in the bulk and near the walls have different life times and subsequently might require different integration times to adequately reveal coherent structures. Furthermore, the short life times and fast growth of eddies near the wall region might muddy the FTLE field if too long integration times are used. For instance, say that a grid of particles is injected near the wall and currently there is no vortex there, then along the integration a vortex might quickly grow and create high FTLE ridges, yet they were not there at the injection time. This leads to the risk of having fast growing vortices with short life times superimpose themselves backward or forward in time if too long integration times are being used. Another problem with the near wall region is that several vortices might grow and die out during the integration time that is needed to reveal structures in the bulk, so that several vortices are superimposed on top of each other in the FTLE field. A closer inspection of the FTLE field

from LES simulations, e.g. see figures 18 or 20, show that the FTLE field in the near wall region seems to have ridges overlapping and crossing each other, maybe the result of several vortices having been formed and died out during the integration time.

The good overlap of the attracting LCS with TKE and the velocity field show, which can be seen in figure 21 and 22, that the method is worth investigating further to create a method to construct three dimensional volumes such that the amount of TKE for instance can be calculated and compared to Eulerian methods. If this was possible in a meaningful way it would give a method to compare how much TKE is captured by the LCS and the Q-criterion as the structures produced by the two methods are typically different in location and size. If it is not possible then that would redefine the meaning of what a turbulent structure is, and that would be perhaps even more interesting. As such, future work should be focused on this part.

References

Andersson, B., Andersson, R., Håkansson, L., Mortensson, M., Sudiyo, R., van Wachem, B. (2011). Computational Fluid Dynamics for Engineers. Cambridge, New York., Cambridge University Press.

Andersson, R. and B. Andersson (2006a). "On the breakup of fluid particles in turbulent flows." Aiche Journal **52**(6): 2020-2030.

Andersson, R. and B. Andersson (2006b). "Modeling the breakup of fluid particles in turbulent flows." Aiche Journal **52**(6): 2031-2038.

Brunton, S. L. and C. W. Rowley (2010). "Fast computation of finite-time Lyapunov exponent fields for unsteady flows." Chaos **20**(1).

Chakraborty, P., S. Balachandar, et al. (2005). "On the relationships between local vortex identification schemes." Journal of Fluid Mechanics **535**: 189-214.

Crowe, C. T., Schwarzkopf, J. D., Sommerfeld M., Tsuji, Y. (2011). Multiphase Flows with Droplets and Particles. Boca Raton, FL., CRC Press.

Devenport, W. J., M. C. Rife, et al. (1996). "The structure and development of a wing-tip vortex." Journal of Fluid Mechanics **312**: 67-106.

Dubief, Y. and F. Delcayre (2000). "On coherent-vortex identification in turbulence." Journal of Turbulence **1**: 1-22.

Garnier, N., Adams, N., Sagaut, P. (2009). Large Eddy Simulation for Compressible Flows. Dordrecht; London, Springer.

Ghasempour, F., R. Andersson, et al. (2011). "Multidimensional turbulence spectra - identifying properties of turbulent structures." J. Phys.: Conf. Ser. **318**(4): 1-10.

Green, M. A., C. W. Rowley, et al. (2007). "Detection of Lagrangian coherent structures in three-dimensional turbulence." Journal of Fluid Mechanics **572**: 111-120.

Haller, G. (2001). "Distinguished material surfaces and coherent structures in three-dimensional fluid flows." Physica D **149**(4): 248-277.

Haller, G. (2002). "Lagrangian coherent structures from approximate velocity data." Physics of Fluids **14**(6): 1851-1861.

Haller, G. (2005). "An objective definition of a vortex." Journal of Fluid Mechanics **525**: 1-26.

Haller, G. (2011). "A variational theory of hyperbolic Lagrangian Coherent Structures." Physica D-Nonlinear Phenomena **240**(7): 574-598.

Olcay, A. B. and P. S. Krueger (2008). "Measurement of ambient fluid entrainment during laminar vortex ring formation." Experiments in Fluids **44**(2): 235-247.

Peacock, T. and J. Dabiri (2010). "Introduction to Focus Issue: Lagrangian Coherent Structures." Chaos **20**(1).

Pope, S. B. (2000). Turbulent Flows. Cambridge, Cambridge University Press.

Shadden, S. C. (2011). Lagrangian Coherent Structures, in Transport and Mixing in Laminar Flows: From Microfluidics to Oceanic Currents. R. Grigoriev. Weinheim, Germany, Wiley-VCH Verlag GmbH & Co. KGaA.

Shadden, S. C., J. O. Dabiri, et al. (2006). "Lagrangian analysis of fluid transport in empirical vortex ring flows." Physics of Fluids **18**(4).

Shadden, S. C., F. Lekien, et al. (2005). "Definition and properties of Lagrangian coherent structures from finite-time Lyapunov exponents in two-dimensional aperiodic flows." Physica D-Nonlinear Phenomena **212**(3-4): 271-304.

Appendix

A.1 Calculation of FTLE

The main program for calculating the FTLE field from exported CFD solution data is `LITS_FTLE.m` (LITS stands for Lagrangian investigation of turbulent structures) that utilizes one sub routine called `lyapunov3D.m`. The solution data is exported from fluent as ASCII files and then read into MATLAB.

LITS_FTLE.m

```
%-------------------------------------------------------------------------%
%      Calculate 3D FTLE field of solution data obtained from Fluent      %
%-------------------------------------------------------------------------%
% matrix columns of sol_data:
% 1 nodenumber
% 2 x-coordinate
% 3 y-coordinate
% 4 z-coordinate
% 5 x-velocity
% 6 y-velocity
% 7 z-velocity
%-------------------------------------------------------------------------%
%% create injection grid
% set grid-resolution
grid_res_xy=1.4e-4;
grid_res_z=3e-4;
x=[-0.013 0.001];
y=[-0.021 -0.0075];
z=[0.11 0.145];
nx=floor((x(2)-x(1))/grid_res_xy)+1;
ny=floor((y(2)-y(1))/grid_res_xy)+1;
nz=floor((z(2)-z(1))/grid_res_z)+1;
% make interval even
x(2)=x(1)+(nx-1)*grid_res_xy;
y(2)=y(1)+(ny-1)*grid_res_xy;
z(2)=z(1)+(nz-1)*grid_res_z;
% set interval of all three space dimensions
x0=linspace(x(1),x(2),nx)';
y0=linspace(y(1),y(2),ny)';
z0=linspace(z(1),z(2),nz)';
% create vectors of all grid points
x=x0*ones(1,ny);
x=x(1:end)';
x=x*ones(1,nz);
x=x(1:end)';
y=ones(nx,1)*y0';
y=y(1:end)';
y=y*ones(1,nz);
y=y(1:end)';
z=ones(nx,1)*z0';
z=z(1:end)';
z=ones(ny,1)*z';
z=z(1:end)';
Np=nx*ny*nz; % no. particles
check=sqrt(x.^2+y.^2)>=0.025;
s=sum(check);
if s>0
    error('particles sided outside of domain')
end
clear x0 y0 z0 check s grid_res_xy grid_res_z
%% calculate particle tracks
```

```
tstart=5300; % time step where advection begins
tend=4801; % and the last time step
% create vectors to store particle locations
Nt=tstart-tend+1; % no. time steps
X=zeros(Np,3);
Y=X;
Z=X;
X(:,end)=x;
Y(:,end)=y;
Z(:,end)=z;
X(:,2)=x;
Y(:,2)=y;
Z(:,2)=z;
t=-0.001; % length of time step [s]
h=waitbar(0,'Calculating flow map...');
for tstep=tstart:-1:tend
    name=['solution_data-' num2str(tstep)];
    sol_data0=dlmread(name,'',1,0);
    [~, m]=sort(sol_data0(:,4));
    sol_data0=sol_data0(m,:); % arrange according to z-value
    % create interpolation function
    x0=sol_data0(:,2);
    y0=sol_data0(:,3);
    z0=sol_data0(:,4);
    vx0=sol_data0(:,5);
    vy0=sol_data0(:,6);
    vz0=sol_data0(:,7);
    VIx0=TriScatteredInterp(x0,y0,z0,vx0);
    VIy0=TriScatteredInterp(x0,y0,z0,vy0);
    VIz0=TriScatteredInterp(x0,y0,z0,vz0);
    % calculate relative position of z-coordinates within periodic boundary
    Zrel=(Z(:,2)./0.2-floor(Z(:,2)./0.2))*0.2;
    % interpolate new positions
    X(:,1)=X(:,2)+t*VIx0(X(:,2),Y(:,2),Zrel);
    Y(:,1)=Y(:,2)+t*VIy0(X(:,2),Y(:,2),Zrel);
    Z(:,1)=Z(:,2)+t*VIz0(X(:,2),Y(:,2),Zrel);
    X(:,2)=X(:,1);
    Y(:,2)=Y(:,1);
    Z(:,2)=Z(:,1);
    waitbar((tstart+1-tstep)/(tstart+1-tend))
    clear x0 y0 z0 vx0 vy0 vz0 VIx0 VIy0 VIz0 sol_data0 name m Zrel
end
run=1;
delete(h)
name1=['flow_map-bt-' num2str(tstart) '-x-' num2str(run) '.txt'];
name2=['flow_map-bt-' num2str(tstart) '-y-' num2str(run) '.txt'];
name3=['flow_map-bt-' num2str(tstart) '-z-' num2str(run) '.txt'];
save(name1,'X','-ascii','-double')
save(name2,'Y','-ascii','-double')
save(name3,'Z','-ascii','-double')
clear i h tstep tstart tend tcrit t name1 name2 name3 run
%% create flow map
flow_map=zeros(Np,3,2);
flow_map(:,:,1)=[X(:,end) Y(:,end) Z(:,end)];
flow_map(:,:,2)=[X(:,1) Y(:,1) Z(:,1)];
%% create index vectors
x_index=zeros(Np,2);
x_index(:,1)=(1:Np)';
x_index(:,2)=(1:Np)';
y_index=x_index;
z_index=x_index;
for i=1:nx:Np-nx+1
    x_index(i:i+nx-1,1)=x_index(i:i+nx-1,1)-[0; ones(nx-1,1)];
```

```
    x_index(i:i+nx-1,2)=x_index(i:i+nx-1,2)+[ones(nx-1,1); 0];
end
for j=1:nx*ny:Np-nx*ny+1
    y_index(j:j+nx*ny-1,1)=y_index(j:j+nx*ny-1,1)-[zeros(nx,1); nx*ones(nx*ny-
nx,1)];
    y_index(j:j+nx*ny-1,2)=y_index(j:j+nx*ny-1,2)+[nx*ones(nx*ny-nx,1);
zeros(nx,1)];
end
z_index(nx*ny+1:Np,1)=z_index(nx*ny+1:Np,1)-nx*ny*ones(Np-nx*ny,1);
z_index(1:Np-nx*ny,2)=z_index(1:Np-nx*ny,2)+nx*ny*ones(Np-nx*ny,1);
clear i j
%% calculate FTLE
T=Nt*0.001;
FTLE=lyapunov3D(flow_map,Np,x_index,y_index,z_index,T);
clear T
```

lyapunov3D.m

```
function FTLE=lyapunov3D(flow_map,Np,x_index,y_index,z_index,T)
def_grad=zeros(3,3,Np); % matrix to store gradient for each particle
FTLE=zeros(Np,1); % vector to store FTLE:s
FTLEindex=zeros(Np,1);
% calculate def_grad by finite differencing
for k=1:Np
    xyij=[x_index(k,:); y_index(k,:); z_index(k,:)];
    for i=1:3
        for j=1:3
            def_grad(i,j,k)=...
                (flow_map(xyij(j,2),i,2)-flow_map(xyij(j,1),i,2))...
                /(flow_map(xyij(j,2),j,1)-flow_map(xyij(j,1),j,1));
        end
    end
    def_grad(:,:,k)=def_grad(:,:,k)'*def_grad(:,:,k);
    lambda=eig(def_grad(:,:,k));
    lambda_m=sort(lambda(1:end));
    FTLE(k)=1/T*log(sqrt(lambda_m(end)));
End
```

B Nomenclature

CFD	computational fluid dynamics
DNS	direct numerical simulation
FTLE	finite time Lyapunov exponent
LCS	Lagrangian coherent structure
LES	large eddy simulation
TKE	turbulent kinetic energy
$\boldsymbol{e}$	eigenvector
g	gravitational constant
$\boldsymbol{J}$	Jacobian
k	turbulent kinetic energy
P	pressure
r	radius
T	integration time
t	time
U_i	instantaneous velocity of coordinate i
$\overline{U}_i$	resolved large scale instantaneous velocity
$\langle U_i \rangle$	average velocity
u_i	velocity due to turbulence
u_i'	modeled subgrid scale velocity
x, y, z	space coordinates
$\boldsymbol{x}, \boldsymbol{y}$	particle position
Δ	Cauchy-Green deformation tensor
λ	eigenvalue
ν	viscosity
ρ	density
σ	FTLE
Φ	flow map
φ	potential field
Ω	domain
$\boldsymbol{\Omega}$	symmetric invariant of $\boldsymbol{\nabla} U$
$\boldsymbol{\nabla}$	gradient